Supplemental Figure 1: Flow cytometry gating strategy for CCR/CXCR homing receptors

First, we discriminated cells based on size scatter and, after exclusion of doublet cells and dead cells, as well as non T cells using the dump channel (staining for CD14, CD15, CD16 and CD19), we analyzed T cell markers. Hence, we gated on $CD4^+$ and $CD8^+$ T cells to analyze distinct subsets of naïve or effector/memory cells using CD45RA and CCR7 mAbs. In each subset, we evaluated the percentage of positive cells for each homing receptor. To evaluate these 9 receptors, we stained cells with one of three 3 different staining cocktails, the first one containing CRTH2, CCR6, CCR10, CXCR3 mAbs (9 colors), and the second and third, with CXCR5, CD103, CCR9 mAbs and CLA, CCR10, CXCR4 mAbs respectively (each 8 colors). An exemplification of the adopted appropriate gating strategy is depicted.

Supplemental Figure 2: Overall survival of 57 MMel studied for CCR and CXCR markers.
Kaplan Meier curves of the three independent cohorts pooled together (patients characteristics and statistics for prognosis parameters presented in Suppl. Table 2) and analyzed for overall survival from diagnosis (A) or from blood sampling for CCR and CXCR studies (B).

Supplemental Figure 3: Correlations between TNs, TCMs, TEMs, TEMRAs $CD4^+$ and $CD8^+$ T cells.
A. Distributions of correlation coefficients between the 4 subpopulations (TNs, TCMs, TEMs and TEMRAs) of the indicated flow cytometry parameters (indicated on y-axis). Dashed lines correspond to the 0.05, 0.01 and 0.001 *P*-significance levels. Correlation matrices from the 20 groups were found to differ from an identity matrix ($P < 10^{-20}$, Bartlett's test). B. Distributions of correlation coefficients between $CD4^+$ and corresponding $CD8^+$ T lymphocytes. Upper panel: 4 subpopulations (TNs, TEMRAs, TEMs, TCMs) for each family. Lower panel: double positive cells. Dashed lines correspond to the 0.05, 0.01 and 0.001 *P*-significance levels. The RV coefficient (given in parentheses) between the $CD4^+$ and $CD8^+$ sub-population matrices indicates a poor correlation index between CXCR4 and CD103 markers. Of note, each sample was split into two batches that were stained with the same CCR10 mAb but different additional markers and then subjected to flow cytometry. Therefore, CCR10 was measures twice and featured on the graphs as CCR10 and CCR10.2. Note that these two CCR10 measurements correlated among each other.

Supplemental Figure 4: Increase in circulating proportions of $CD4^+CD103^+$ TNs associated with liver metastases.
A. ROC curves depicting the predictive properties of CD103 on $CD4^+$TNs determined in patients presenting liver metastases (N=19) in multimetastatic patients (N=36) and associated area under the curve (AUC). B. Distribution of the expression of CD103 on $CD4^+$ TNs in each subset of

patients, stratified according to the diagnosis of liver metastases. C-D. Distributions of $CD103^+$ $CD4^+$ T cells coexpressing CXCR5 (C) or CCR9 (D) receptors in MMel patients who were known for the ulceration status (N=18). Each point represents one patient specimen and the total number is indicated for all subpopulations studied. Statistical analyses were performed by logistic (A) and beta regression (B-D) modeling. *P* values are indicated.

Supplemental Figure 5: CLA expression on T cells is weakly associated with disease dissemination.

A-B. CLA expression on $CD8^+$ (A) and $CD4^+$ (B) TEMRAs (upper panels) and TCMs (lower panels) is depicted for HV, for patients presenting with only cutaneous/LN metastases (Cut+LN), with additional lung involvement (Lu), with disseminated diseases (Multi) and with distant metastases plus lung involvement (Multi+Lu) at the time of inclusion in one of the three protocols described in M&M. C-D. Match-paired comparison between CLA expressions (performed in flow cytometry on fresh tissues) in all $CD8^+$ (C) and $CD4^+$ (D) T cell subsets from blood (B) and tumors (T) at surgery in the prospective cohort of 20 patients with MMel. Each point represents one patient specimen and the total number is indicated for all subpopulations studied. Statistical analyses were performed by beta regression (A-B) and linear mixed effects (C-D) modeling. Raw *P* values are indicated.

Supplemental Figure 6: $CD4^+CXCR4^+$ TEMRAs accumulated in tumor LN.

A-B. CXCR4 expression on $CD4^+$TEMRAs (A) and TCMs (B) is depicted for HV, for patients presenting with only cutaneous/LN metastases (Cut+LN), with additional lung involvement (Lu), with disseminated diseases (Multi) and with distant metastases plus lung involvement (Multi+Lu) at the time of inclusion in one of the three protocols described in M&M C. Match-paired comparison between CXCR4 expressions (performed by flow cytometry on fresh tissues) in all $CD4^+$ T cell subsets from blood (B) and tumors (T) at surgery in the prospective cohort of 20 patients with MMel. Each point represents one patient specimen and the total number is indicated for all subpopulations studied. Statistical analyses were performed by beta regression (A-B) and linear mixed effects (C) modeling. Raw *P* values are indicated.

Supplemental Figure 7: CXCR5 expression decreases during lung metastases.

A-B. CXCR5 expression on $CD4^+$ TEMRAs (A) and $CD4^+CCR9^+$ T cells (B) is depicted for HV, for patients presenting with only cutaneous/LN metastases (Cut+LN), with additional lung (Lu) involvement, with disseminated diseases (Multi) and with metastases in lung and other distant organs (Multi+Lu) at the time of inclusion in one of the three protocols described in M&M C. Match-paired comparison between CXCR5 expressions (performed in flow cytometry on fresh

tissues) in all $CD4^+$ T cell subsets from blood (B) and tumors (T) at surgery in the prospective cohort of 20 patients with MMel D. $CD4^+CXCR5^+$ T cell cytokine profile. Flow cytometry-guided sorting based on CXCR5/CD103 expression in blood $CD4^+$ T cells in one representative patient (out of two yielding similar results, means from duplicate wells) to analyze cytokine release after a 40 hr CD3/CD28 beads-driven stimulation. Each point represents one patient specimen and the total number is indicated for all subpopulations studied. Statistical analyses were performed by beta regression (A-B) and linear mixed effects (C) modeling. Raw *P* values are indicated.

Supplemental Figure 8. CRTH2 expression and distant metastases.

Flow cytometric analyses of double positive $CRTH2^+CCR10^+$ (A), $CCR10^+CXCR3^+$ (B) and $CRTH2^+CXCR3^+$ (C) $CD4^+$ T cells in 57 MMel patients according to their metastatic pattern at sampling. Each point represents one patient specimen and the total number is indicated for all subpopulations studied. Statistical analyses were performed by beta regression modeling. Raw *P* values are indicated.

Supplemental Figure 9. CD103 expression by $CD4^+$ TCMs associated with distant metastases.

A. CD103 expression on $CD4^+$ TCMs is depicted for healthy volunteers (HV), for patients presenting with only cutaneous/lymph node (Cut+LN) metastases, with additional lung (Lu) involvement, with disseminated diseases (Multi) and with distant metastases plus lung involvement (Multi+Lu) at the time of inclusion in one of the three protocols described in M&M. B. $CD4^+CD103^+$ T cell cytokine profile. Flow cytometry-guided sorting based on the CXCR5/CD103 expression of blood $CD4^+$ T cells in one representative patient (out of two yielding similar results, means from duplicate wells) to analyze cytokine release after a 40 hr CD3/CD28 beads-driven stimulation.. C. Match-paired comparison between CD103 expression (performed by flow cytometry on fresh tissues) in all $CD4^+$ T cell subsets from blood (B) and tumors (T) of patients at surgery in the prospective cohort of 20 patients with MMel. D. Flow cytometry analysis of CD103 and Foxp3 expression gating on $CD4^+$ T cells in one representative example out of three. Each point represents one patient specimen and the total number is indicated for all subpopulations studied. Statistical analyses were performed by beta regression (A) and linear mixed effects (C) modeling. Raw *P* values are indicated.

Suppl. Figure 1

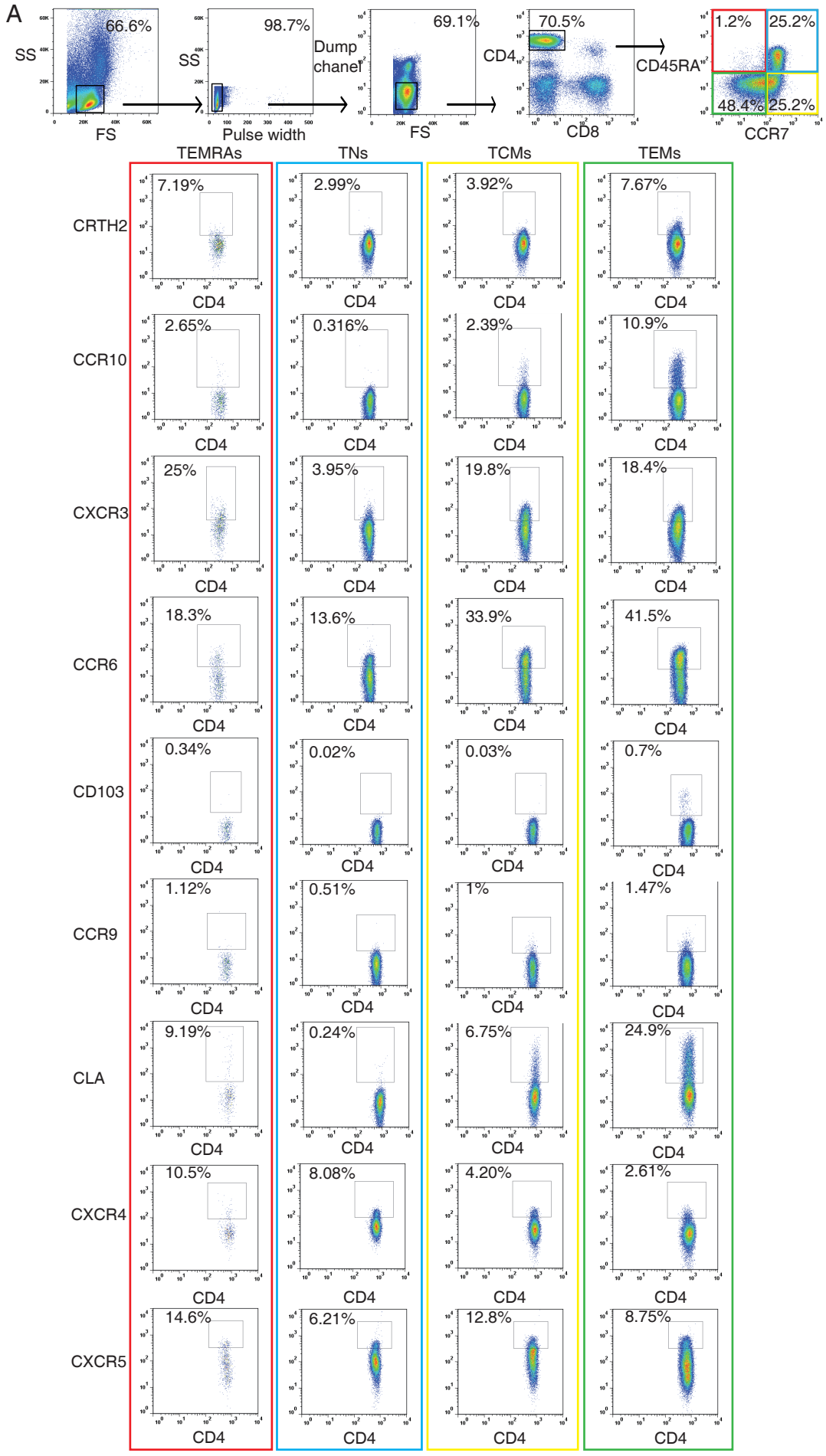

Suppl. Figure 2

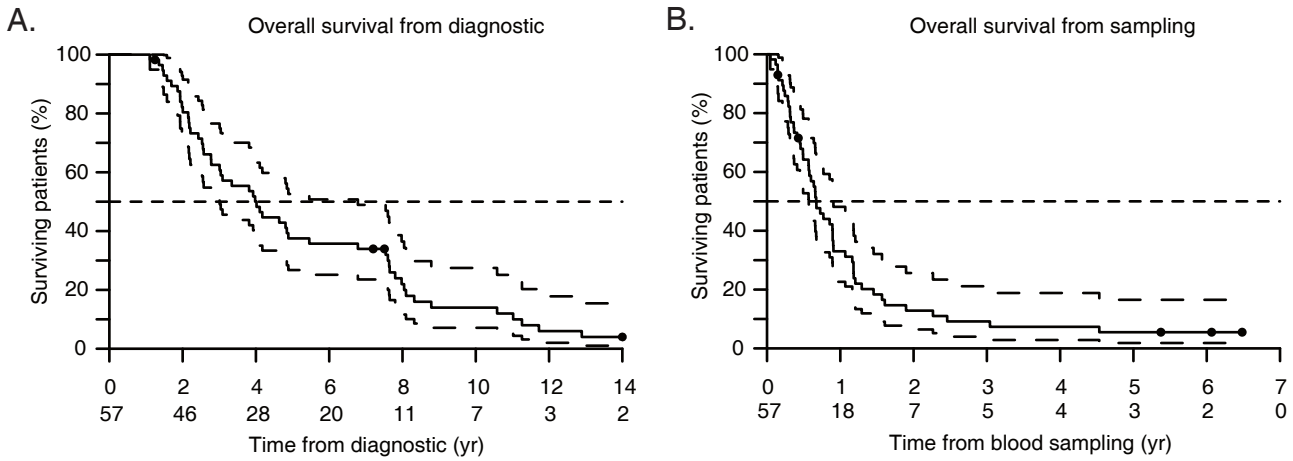

Suppl. Figure 3

A.

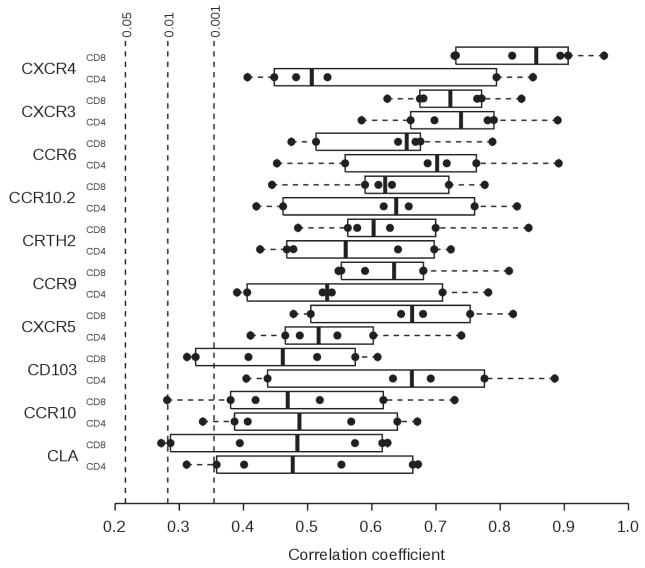

B.

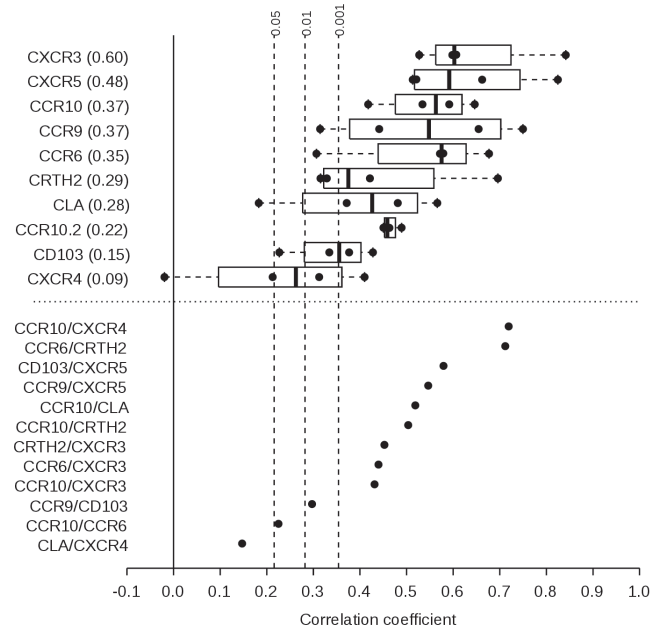

Suppl. Figure 4

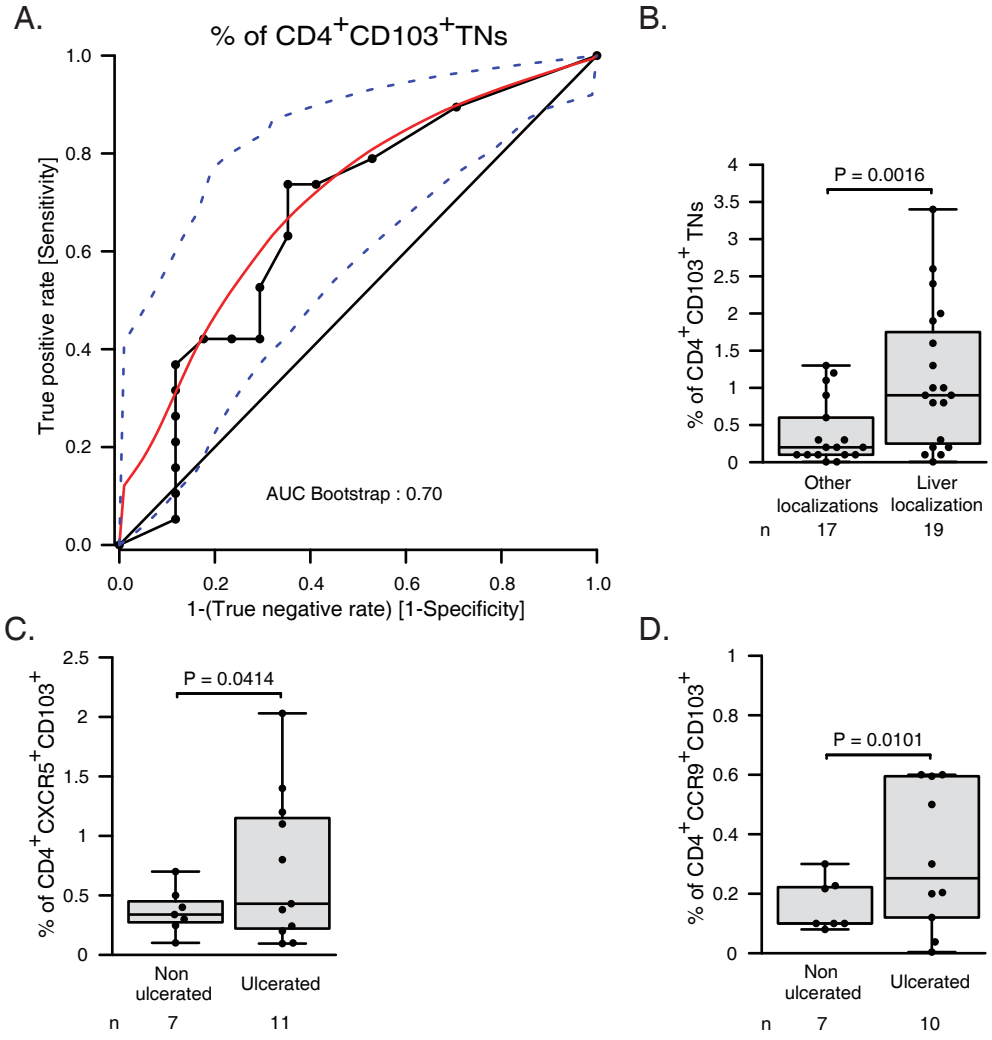

Suppl. Figure 5

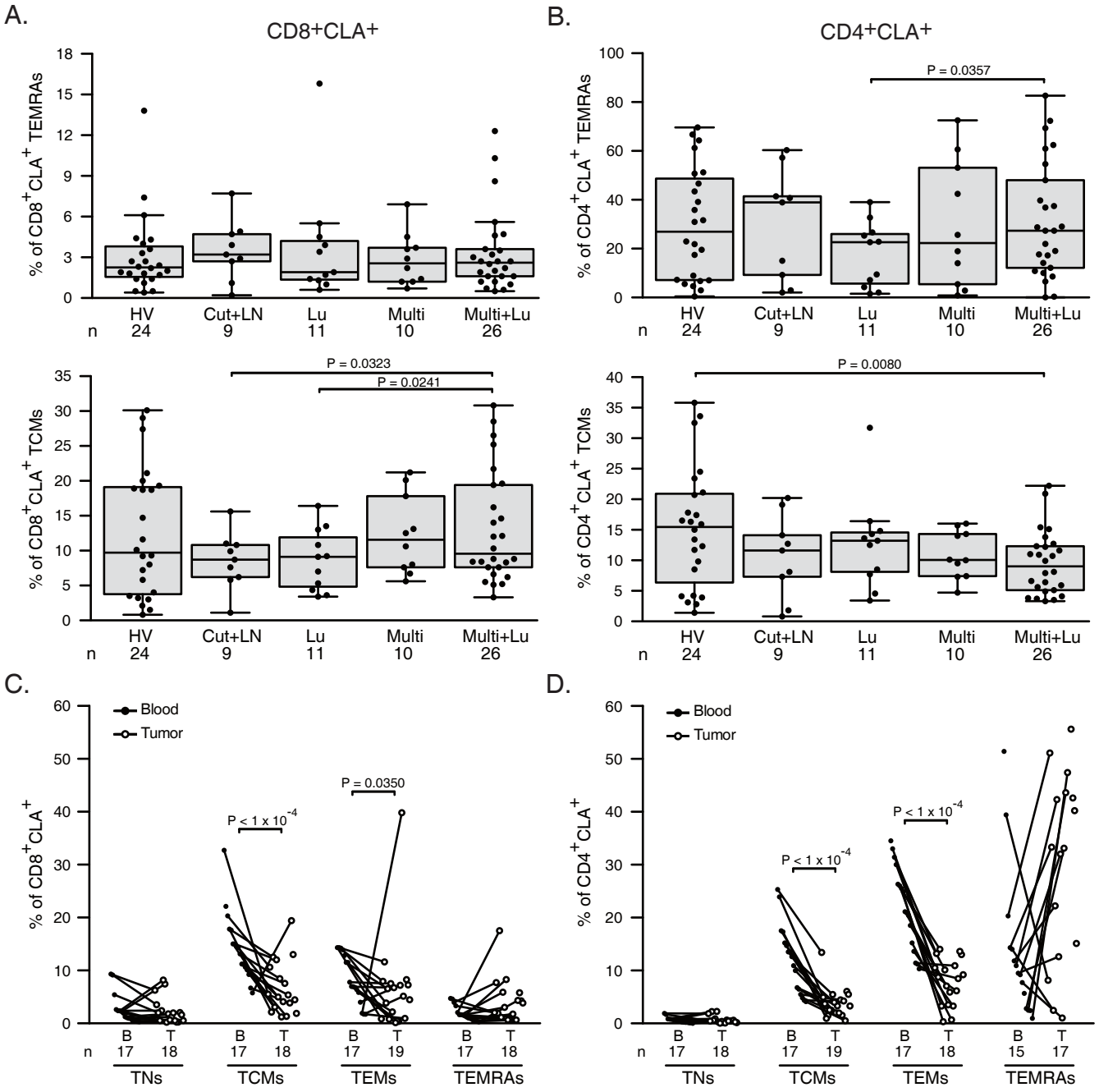

Suppl. Figure 6

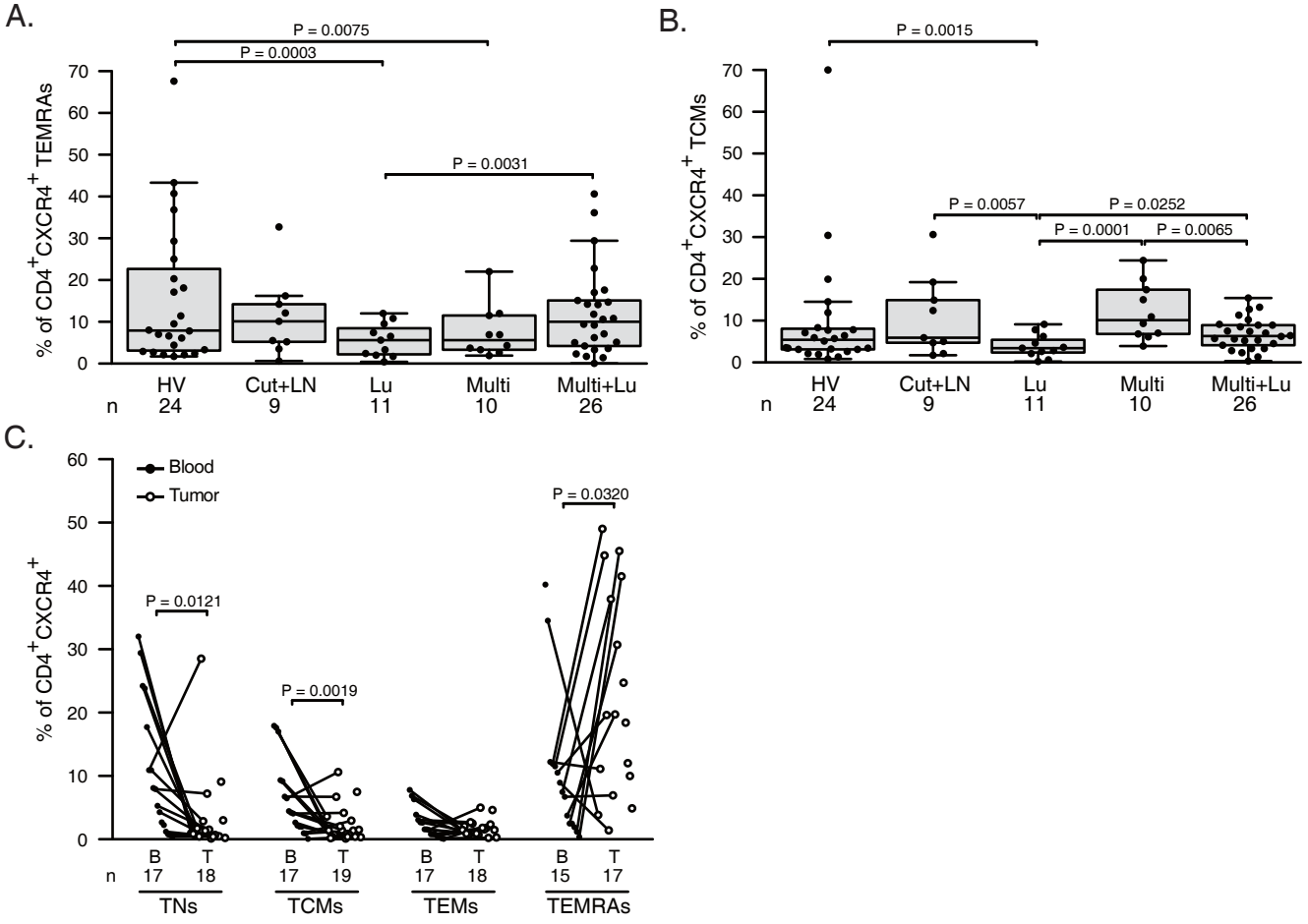

Suppl. Figure 7

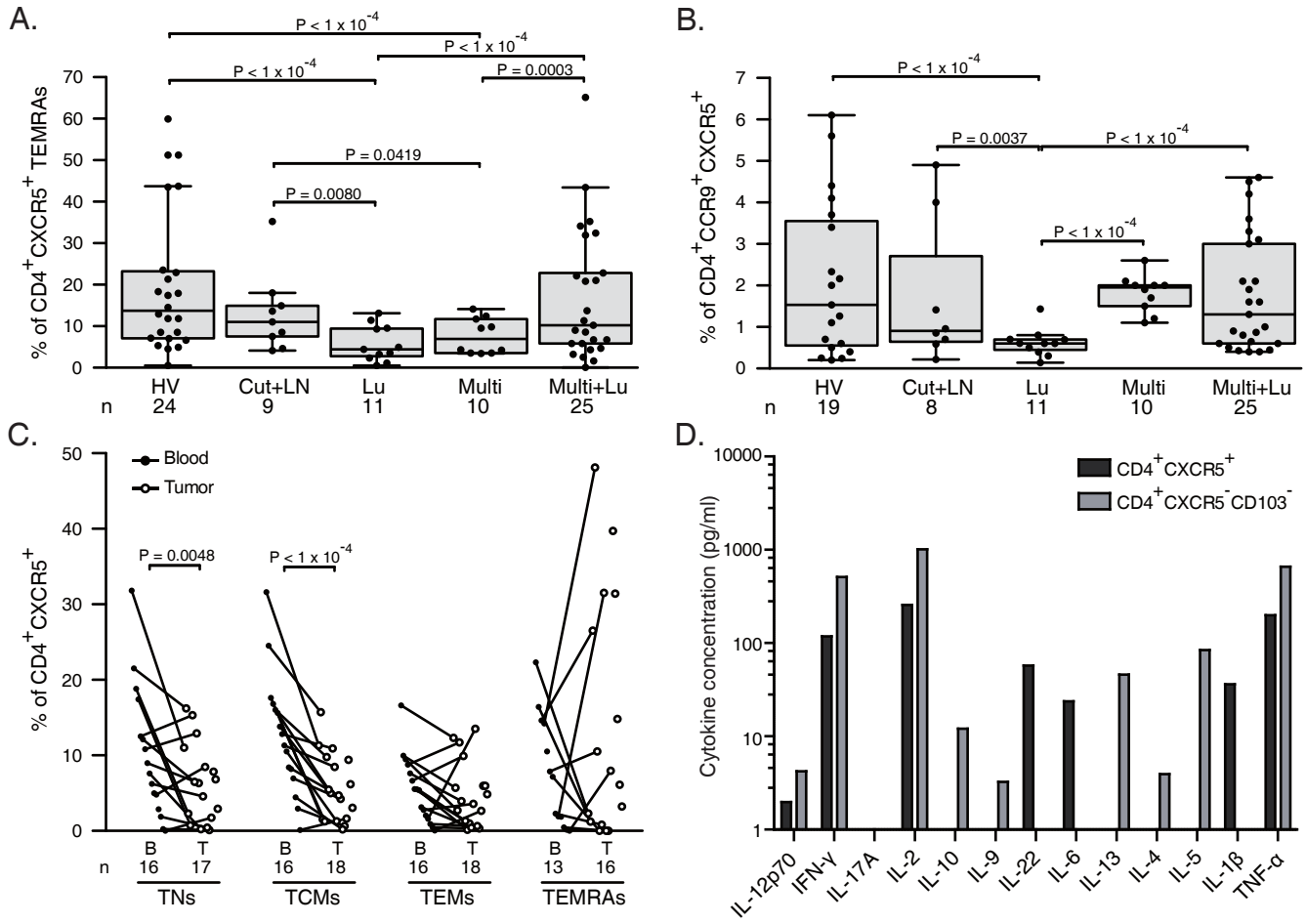

Suppl. Figure 8

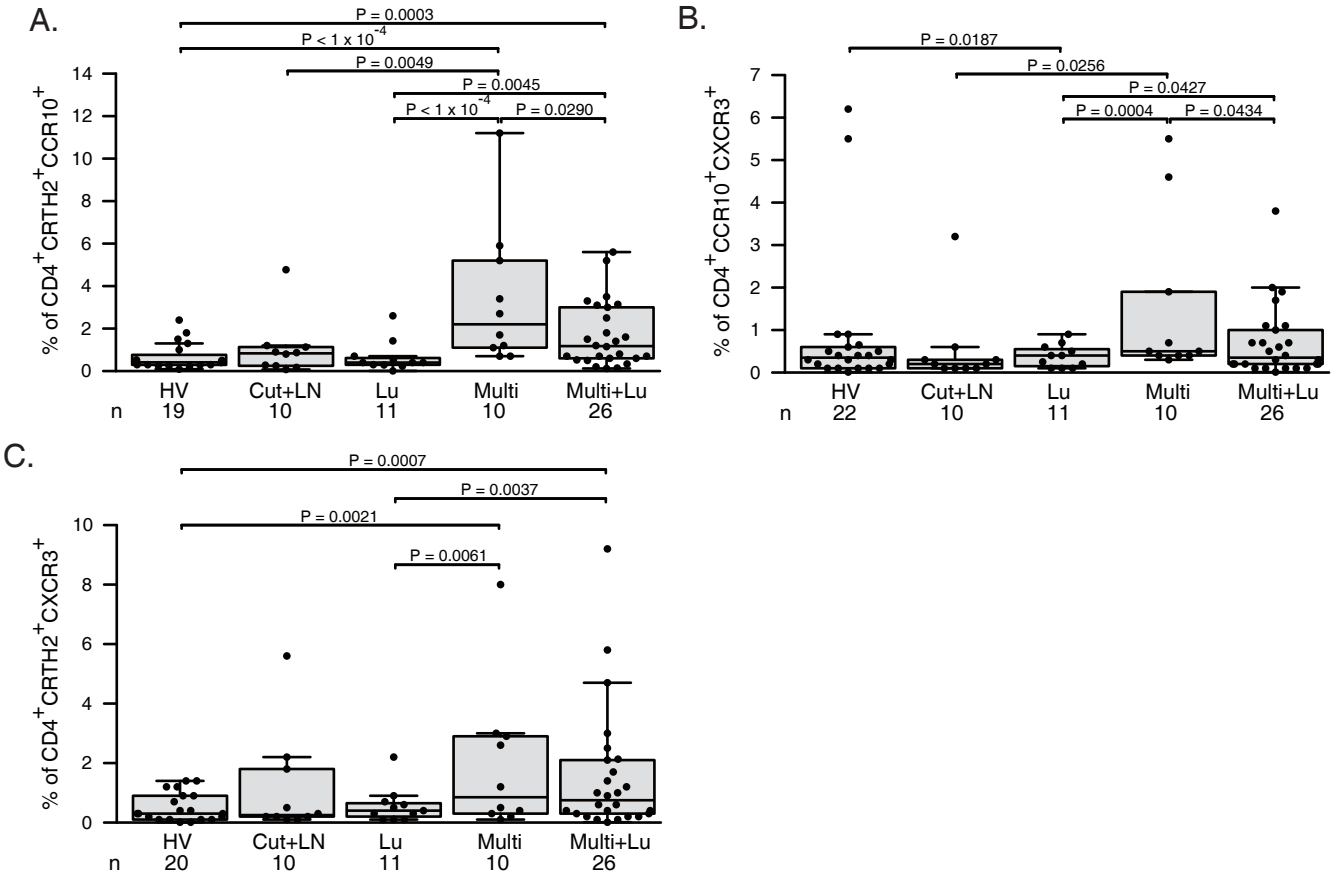

Suppl. Figure 9

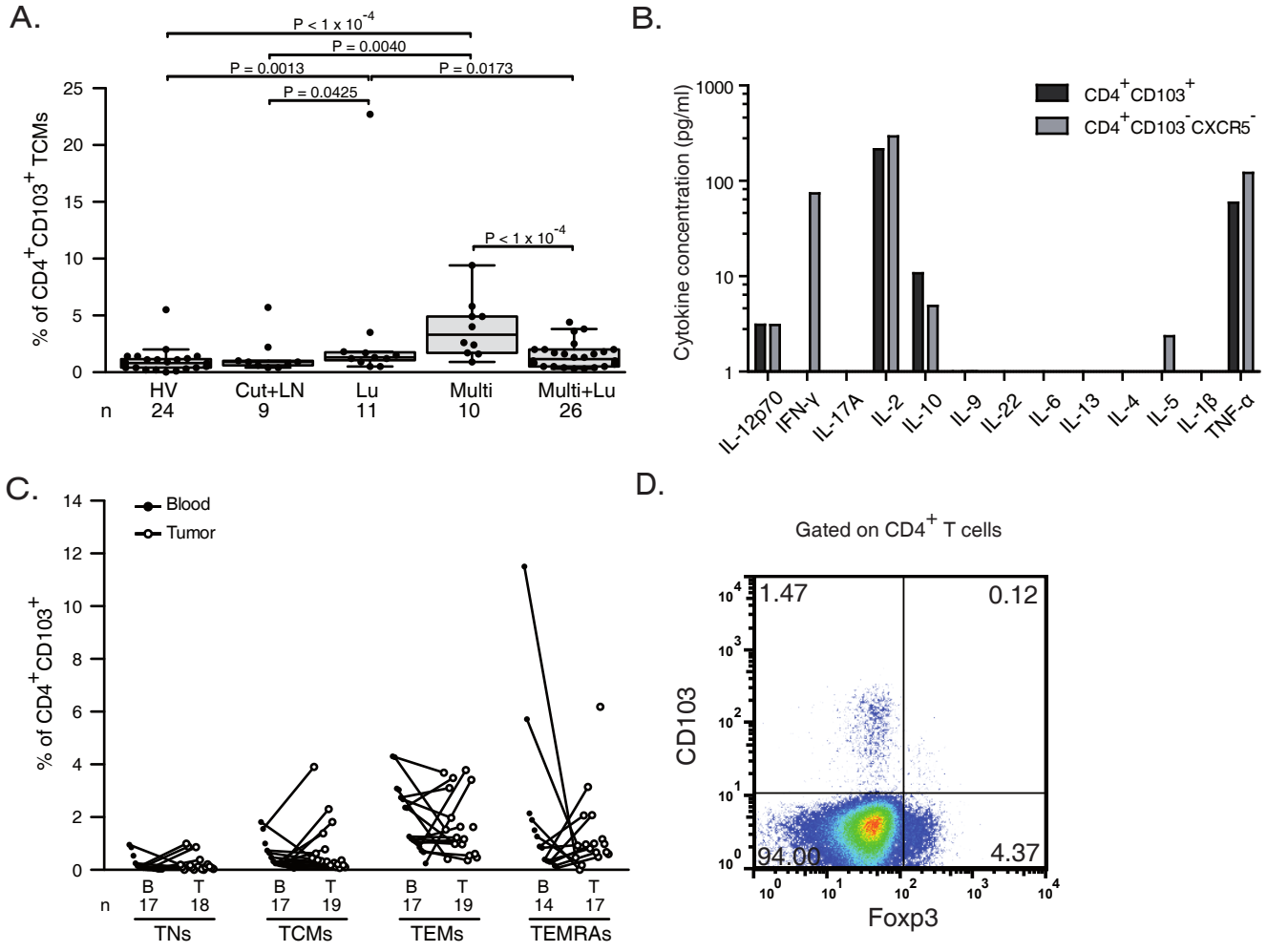

Supplemental Table 1: Characteristics of mAbs used in this study

Specificity	*Fluorochrome*	*Ab clone*	*Company*	*Reference*
CXCR5	AF488	RF8B2	BD	558112
CLA	FITC	HECA-452	BD	561987
CRTH2	FITC	BM16	BD	561659
CD103	PE	Ber-ACT8	BD	550260
CCR10	PE	314305	R&D	FAB3478P
CD4	PE-CF594	RPA-T4	BD	562281
CD8	PerCP	SK1	BD	345774
CCR9	PerCP Cy5.5	BL/CCR9	Biolegend	346303
CXCR4	PerCP Cy5.5	12G5	Biolegend	306516
CXCR3	PE Cy7	1C6/CXCR3	BD	560831
CD4	PE Cy7	SK3	BD	557852
CCR7	BV421	G043H7	Biolegend	353208
CD14	V500	M5E2	BD	561391
CD15	V500	HI98	BD	561585
CD16	V500	3G8	BD	561394
CD19	V500	HIB19	BD	561121
CD8b	APC	2ST8.5H7	BD	641058
CCR6	AF647	11A9	BD	560466
CD45RA	APC-H7	HI100	BD	560674
Dead Cells	Yellow	--	Invitrogen	L34959

Supplemental Table 2: Retrospective analysis performed on 3 cohorts gathering 57 MMel patients; impact of clinical parameters on the overall survival from blood sampling

		N [%]	*HR [95 %CI]*	*LRT, P value*
Age (yrs)[A]		44 [13;72]	0.99 [0.97;1.01], *P* = 0.5368	0.38, *P* = 0.5368
Gender	M	29 [50.9]	1	1.11, *P* = 0.2924
	F	28 [49.1]	1.34 [0.77;2.32], *P* = 0.2924	
Breslow (mm) on primary tumor[A]		2.2 [0.0;12.0]	0.95 [0.84;1.09], *P* = 0.4568	0.55, *P* = 0.4568
Stage	III	10 [17.5]	1	6.69, *P* = 0.0097
	IV	47 [82.5]	2.58 [1.16;5.76], *P* = 0.0097	
Metastases	Skin+LN	10 [17.5]	1	12.49, *P* = 0.0059
	Lung	11 [19.3]	1.94 [0.75;5.04], *P* = 0.1589	
	Miscellaneous	10 [17.5]	5.5 [2;15.11], *P* = 0.0007	
	Miscellaneous+Lung	26 [45.6]	2.65 [1.13;6.24], *P* = 0.0148	
Cohort	IMAIL-2	5 [8.8]	1	0.87, *P* = 0.6485
	Ludwig	13 [22.8]	0.64 [0.23;1.79], *P* = 0.3989	
	SORAFTEM	39 [68.4]	0.8 [0.32;2.02], *P* = 0.6466	
LDH (UI/L)[A]		230 [98;1027]	1 [1;1], *P* = 0.7187	0.13, *P* = 0.7187

[A]Mean[Min;Max]

Supplemental Table 3: Chemokine receptor analysis performed on 4 different cohorts of 47 MMel patients treated with ipilimumab; description of main clinical parameters

			All patients - N [%]	*French Cohort - N [%]*	*Italian Cohort – N [%]*	*American Cohort – N [%]*	*German Cohort – N [%)*
Gender	M F		28 [59.6] 19 [40.4]	12 [54.5] 10 [45.5]	6 [60.0] 4 [40.0]	7 [63.6] 4 [36.4]	3 [75.0] 1 [25.0]
Age (yrs)[A]			61 [24;91]	60 [82;37]	55.6 [81;24]	65 [91:41]	66.8 [75;53]
Stage	III IV		5 [10.6] 42 [89.4]	4 [18.2] 18 [81.8]	1 [10.0] 9 [90.0]	0 [0.0] 11 [100.0]	0 [0.0] 4 [100.0]
LDH (UI/L)[A]			356 [2510;128]	434 [2510;135]	347 [540;144]	238 [477;135]	279 [558;128]
Dose of Ipilimumab (mg/kg)	3 10		41 [87.2] 6 [12.8]	16 [72.7] 6 [27.2]	10 [100.0] 0 [0.0]	11 [100.0] 0 [0.0]	4 [100.0] 0 [0.0]
Concomitant therapy	No Yes		34 [72.3] 13 [27.7]	13 [59.1] 9 [40.9][B]	10 [100.0] 0 [0.0]	11 [100.0] 0 [0.0]	0 [0.0] 4 [100.0][C]
Prior therapy	No Yes 	 Radiotherapy/Chemotherapy Tyrosine kinase inhibitor[D] Immunotherapy[E]	10 [21.3] 37 [78.7] 29 [61.7] 10 [21.3] 12 [25,5]	9 [40.9] 13 [59.1] 7 [31.8] 5 [22.7] 6 [27.2]	1 [10.0] 9 [90.0] 8 [80.0] 3 [30.0] 3 [30.0]	0 [0.0] 11 [100.0] 11 [100.0] 2 [18.2] 2 (18.2]	0 [0.0] 4 [100.0] 3 [75.0] 1 [25.0] 2 [50.0]
Clinical response at 3 months	NR R 	 Complete Response Partial Response Stable Disease	29 [61.7] 18 [38.3] 1 [2.1] 7 [14.9] 10 [21.3]	12 [54.5] 10 [45,5] 1 [4.6] 7 [31.8] 2 [9.1]	6 [60.0] 4 [40.0] 0 [0.0] 0 (0.0] 4 (40.0]	7 [63.6] 4 [36.4] 0 [0.0] 0 [0.0) 4 [36.4]	4 [100.0] 0 [0.0] 0 [0.0] 0 (0.0] 0 [0.0]

[A]Mean[Min;Max]
[B]Patients were treated with local radiotherapy.
[C]Patients received between 7 and 8 intratumoral injection of IL-2 (9MUI/injection).
[D]Vemurafenib, Dabrafenib, Pazopanib, Lenvatinib.
[E]IL-2, Interferon, anti-PD1, anti-CTLA-4

Supplemental Table 4: Summary of the principal findings of this paper

Surface marker	Subset of T cells	Correlation with metastatic dissemination patterns	Prognostic impact	Predictive impact
CCR6	CD4 TEMs, TCMs,TEMRAs CD8 TNs, TEMs, TCMs	Reduction correlates with cutaneous and lymph node metastases	Poor prognosis if expressed by CD8 TEMs	
CXCR3	CD4, CD8, TNs CD4, CD8, TEMs CD4 TCMs CD4 TEMRAs	Reduction correlates with cutaneous and lymph node metastases	Good prognosis if expressed by CD4 TEMs	
CXCR4	CD4 TEMs,TCMs CD8 TNs, TEMs, TCMs, TEMRAs	Reduction correlates with lung metastases		
CXCR5	CD4 TNs, TCMs, TEMRAs CD8 TNs, TCMs	Reduction correlates with lung metastases		
CCR9		Reduction correlates with lung metastases	Good prognosis if expressed by CD8 TNs	
CD103	CD4 TNs CD4 TEMs, TEMRAs, TCMs, TNs	Increase correlates with hepatic metastasis Increase correlates with visceral metastasis		
CCR9/CD103	CD4	Increase in ulcerated melanoma		
CRTH2	CD4 TEMs CD8 TCMs, TEMs	Increase correlates with visceral metastases		
CCR10	CD4 TEMs CD4 and CD8 TNs, TCMs	Increase Increase correlates with visceral metastases	Poor prognosis	
CLA	CD8 TEMs	Increase after one injection of ipilimumab		Increase predicts ipilimumab response
CCR10/CLA	CD4 TEMs		Poor prognosis	